Published in final edited form as:
Nano Lett. 2011 April 13; 11(4): 1469–1476. doi:10.1021/nl104079r.

Impact of Local versus Global Ligand Density on Cellular Adhesion

Janosch A. Deeg[1], **Ilia Louban**[1], **Daniel Aydin**[1], **Christine Selhuber-Unkel**[2], **Horst Kessler**[3], and **Joachim P. Spatz**[1]

Joachim P. Spatz: spatz@mf.mpg.de

[1]Department of New Materials and Biosystems, Max Planck Institute for Metals Research, Heisenbergstraße 3, 70569 Stuttgart, Germany & Department of Biophysical Chemistry, University of Heidelberg, Germany

[2]Zoological Institute, University of Kiel, Germany

[3]Institute for Organic Chemistry und Biochemistry, Lehrstuhl II, Technical University of Munich, Lichtenbergstraße 4, 85747 Garching, Germany

Abstract

$\alpha_v\beta_3$ integrin-mediated cell adhesion is crucially influenced by how far ligands are spaced apart. To evaluate the impact of local ligand density versus global ligand density of a given surface we used synthetic micro-nanostructured cell environments with user-defined ligand spacing and patterns to investigate cellular adhesion. The development of stable focal adhesions, their number and size as well as the cellular adhesion strength proved to be influenced by local more than global ligand density.

Keywords

Integrin; Focal Adhesion; ECM; Micro-Nanostructures; Biointerfaces; Single Cell Force Spectroscopy (SCFS)

Introduction

In complex living systems most cells are organized in ensembles held together by the extracellular matrix (ECM), a meshwork of fibrous proteins and polymers. Numerous studies have shown that the properties of the ECM crucially affect the behavior and development of cellular systems at multiple length scales.[1, 2] In effect, this means that nano-sized structures not only influence components that share a common length scale, but can cause changes in the entire organism that is many orders of magnitude larger. Cell experiments with synthetic micro- and nano-environments have revealed the extraordinary capacity of cells to respond to many different environmental parameters such as rigidity, dimensionality, topography and global or local adhesive ligand density.[3, 4] These properties act as extracellular signals that influence cell characteristics like morphology and migration as well as cell responses such as differentiation, proliferation and apoptosis.[3, 5, 6] Through cell-ECM contact sites, so-called focal adhesions (FAs), the cell is able to: (i) spatially recognize biochemical features of its surroundings and organize itself according to these geometrical surface cues, and (ii) process external mechanical stimuli and actively explore mechanical properties of the environment.[7–9] A well studied component of FAs is the

Correspondence to: Joachim P. Spatz, spatz@mf.mpg.de.

transmembrane protein integrin, which plays a crucial role in adhesion and bi-directional signaling across the cell membrane.[10] For the initiation of focal adhesions, integrins and a number of associated proteins (including paxillin, talin and α-actinin among others) must reorganize into well-defined clusters. The development of a focal adhesion starts with the formation of so-called "focal complexes" (usually at the leading edge of migrating cells in lamellipodia), which mature into larger, more stable focal adhesions. These act as anchor points for the cell on the ECM or are disassembled as the lamellipodium withdraws. The spatial organization of integrins, whether as randomly distributed inactive molecules or as well-defined nano- or macroclusters, changes dynamically and is an essential part of how integrins function. Integrin-mediated cellular adhesion has been studied extensively and its importance in development and maintenance of cellular systems has been demonstrated a number of times.[3]

In this project we investigated the $\alpha_v\beta_3$ integrin-based adhesion process of fibroblasts on micro- and nano-patterned surfaces biofunctionalized with integrin ligands. We focused on observing the development and stability of FAs, the cellular spreading behavior and performed molecular-scale measurements of the adhesive forces at work during cell adhesion.

Thus far, many bioactive interfaces have been developed, but most of them are limited in their ability to immobilize molecules of interest to defined spots with single molecule resolution. Initial research concerning the influence of binding sequence density on the spreading behavior and adhesion process of fibroblasts was performed using surfaces with statistically controlled ligand spacing. Successful focal contact formation was prevented when average ligand spacing exceeded 140 nm and spreading of cells was inhibited above an average spacing of 440 nm.[11] Next, a method was introduced by Arnold et al., that allowed for more precise control of extracellular ligand presentation.[12] Highly ordered gold nanoparticles spaced in the two to three digit nanometer range on glass surfaces were used as anchor points for single integrin receptors. A universal length scale ranging between 58–73 nm for ligand spacing was proposed for successful integrin clustering and subsequent cell-ECM adhesion. Additional research using the same substrate system investigated spreading behavior, development of focal adhesions and adhesion strength of fibroblasts. These results confirmed Arnold's initial findings.[12–16] Particularly, the quantification of the forces which are necessary for detaching adherent cells provided new insights as it delivers information on the single cell level. It allows for a direct correlation of FA distribution to the detachment force of individual cells. A fibronectin coated tip-less cantilever of an atomic force microscope was used to rupture adherent fibroblasts from surfaces presenting ligands spaced 28, 50, 90, 103 nm, respectively. Using this approach Selhuber et al. recently found that for spacings ≥ 90 nm focal contact formation was inhibited and the detachment forces or so to speak the "adhesion forces" were significantly decreased compared to spacings ≤ 50 nm. This was also true for the so-called adhesion force density, which relates the detachment force of a cell to their FA area.[14]

Yu Jie Wei et al. were the first who developed a theoretical model explaining the experimental discoveries.[17] In their publication they depict the steps to establishing focal adhesions as following: (1) the cell membrane comes into close contact with a substrate, which causes receptors and ligands to form random molecular bonds that can then act as nuclei of possible focal contacts. These bonds lead to cell membrane stretching and deformation as a 3D bulge is induced; (2) "energy barriers" set by a repulsive bulge pressure (between the cell membrane and substrate) and membrane deformation before the formation of a bound complex can be overcome with the help of thermal undulation. This allows for the establishment of new molecular bonds around focal contact nuclei; (3) the formation of a focal contact is controlled by the capability of the contact zone to spread during its lifetime.

Yu Jie Wei et al. calculated a critical spacing of receptor-ligand bonds of around 39–89 nm for a wide range of repulsive bulge pressures.[17]

Recently de Beer et al. introduced another physical model based on the balance between forces acting on individual ligand-receptor bonds (i.e. the force of the cytoskeletal actin network vs. the antagonistic force from the substrate) and the reaction kinetics of these bonds. In this publication the authors discuss the effects of reducing ligand density based on their calculations and observations. They conclude that expanding the distance between the ligands leads to a substantial increase of force per chemical bond, which in turn causes a greater unbinding rate. In addition, the lower number of available ligands makes rebinding increasingly unlikely. Accordingly, the model states that the establishment of focal adhesions is a function of ligand spacing and applied stress, and proposes three different sets of conditions or regimes: i) a regime in which focal adhesion formation is inhibited; ii) an unstable regime; iii) a stable regime. Assuming an average mechanical stress of 5.5 kPa the corresponding interligand spacings are i) > 93 nm; ii) 76–93 nm; iii) < 76 nm.[18]

All these studies, both experimental and theoretical, collectively agree that small changes in adhesive cues can have a strong influence on the process of cell adhesion. What also unifies the existing research in this field is the fact that adhesion was only investigated on extensive, uniformly patterned substrates which does not allow for the conclusion if the sharp transition of “successful adhesion” to “no adhesion” is due to the amount of ligands in contact with the cell or the distance between individual ligands. In order to answer this question we introduce a novel facet to nanopatterned substrate design by distinguishing between two components of ligand density: how far ligands are spaced apart (specified by local ligand density) and whether the surface is one extensive, uniformly patterned expanse or has a micro-pattern of ligand-coated and ligand-free areas (specified by global ligand density).

We designed several different artificial micro- and nanostructured cell environments and applied various methods to quantitatively evaluate and compare quality characteristics of cell adhesion in dependence of local and global ligand density. Our research is the first to distinguish and selectively evaluate the impact of local ligand density on integrin-mediated cell adhesion.

Block-Copolymer Micelle Nanolithography (BCML), a well-established method based on the self-assembly of macromolecules[21], was employed for the production of surfaces patterned with gold (Au) nano-particles.[20] Gold loaded micelles were deposited on a glass surface by dipcoating. Afterwards the polymer shells of the micelles were removed entirely by hydrogen plasma treatment, leaving quasi-hexagonally ordered nanometer-sized Au-particles on the surface. With this technique interparticle spacing can be varied selectively to distances ranging from 20 to 250 nm.[21] In a second step the global density of the particles was reduced by partially removing them. This was done using a photolithography approach where the extensive nanopatterned surface was covered with a negative photosensitive resist, illuminated through a chromium mask and developed. At this point particles not protected by the resist were removed in an aqueous solution of cysteamine, followed by removal of the protecting resist layer through hydrogen plasma treatment.[19]

This process created patches of nanoparticle arrays separated through empty regions, i.e., micro-nanopatterns as shown in Figure 1. The figure compares an extensive, uniform pattern of Au-nanoparticles and a micro-structured one. Both feature the same interparticle spacing, but the global particle density of the micro-structured pattern is greatly reduced, in other words, the two parameters are now decoupled from each other.

In the next step, the surfaces were biofunctionalized with cellular adhesion ligands. First the area in between the Au-particles was coated with a thin layer of poly(L-lysine)-*g*-

poly(ethylene glycol) (PLL-*g*-PEG), a polymer known for its protein repellency.[22, 23] Next, cyclic-(RGDfK)-thiols were covalently bound to the gold nanoparticles. This ligand was chosen due to the high affinity of RGD to the cellular adhesion receptor $\alpha_V\beta_3$-integrin.[24, 25]

The resulting surfaces display ECM ligands bound to nanoparticles at a ratio of approximately 1:1, thus presenting evenly spaced, individual ligands to which integrins of cells can bind.[19] In contrast to extensive surfaces, which are uniformly patterned with ligands, the micro-nanostructured surface exhibits ligand islands with a diameter of approx. 1.5 μm that are spaced apart approx. 1.7 μm and surrounded by a non-adhesive surface. Such surfaces allow for controlling the local as well as the global density of ligands at appropriate cellular dimensions. [26–28]

The obtained substrate system contains three different extensive, uniformly nanostructured surfaces and one micro-nanostructured surface, which differ in ligand spacing d and densities ρ and ρ. The parameters of the substrates (numbered one through four) are listed in Table 1. The micro-nanostructured surface (**1**) has the same ligand spacing (local ligand density) as the extensive nanopatterned surface (**4),** but features the lowest global ligand density. The ligand spacing of surface **(3)** was chosen to be 74 nm based on previous studies, which described this value to be crucial for cell adhesion.[29] In addition, we chose a surface with ligands spaced wider apart than the critical value of 74 nm (surface (**2**)) and a surface with ligands spaced closer together (surface (**4**)). The application of these four surfaces allowed us to explore the impact of local versus global ligand density for the successful development of stable cellular adhesive clusters.

Adherent cells usually transform from a small, round and sphere-like shape into a large, flat, pancake shape on adhesive surfaces.[11] They optimize their contact area between the environment and the membrane to establish a critical number of contact sites over a certain area.[5, 29, 30] If the surface does not provide adequate adhesion properties, cells remain in an elongated shape exhibiting abundant filopodial structures that serve to explore the substrate.[12] Our cell adhesion experiments were performed with rat embryonic fibroblasts (REF) stably transfected with Paxillin fused to Yellow Fluorescent Protein (REF-YFP-pax). Paxillin is one of several cytosolic plaque proteins associated with integrin in focal adhesions. In our experiments the tagged protein served as a marker to make FAs visible using fluorescence microscopy.[9] Fibroblasts, when brought into contact with an adhesive two-dimensional substrate, spread and establish several contact points, so called focal complexes, which eventually mature into FAs.[11, 31] In contrast, fibroblasts that fail to establish these cell-substrate contacts within a certain time undergo apoptosis.[7]

Based on these facts the following methods (described in further detail below) were applied to analyze values that characterize the quality of cell adhesion on biofunctionalized surfaces (**1–4**):

- **A.** The projected cell area A was measured quantitatively by conventional phase-contrast microscopy after 6 h, 12 h and 24 h of adhesion.
- **B.** The adhesion force F_{ADH} involved in fibroblast-substrate interaction processes was measured quantitatively using single cell force spectroscopy (SCFS) after 12 hours of adhesion. To detach cells from the substrate surface a biofunctionalized cantilever driven by an atomic force microscope (AFM) was utilized. The complete detachment of cells was monitored inside the fluid chamber through phase contrast microscopy performed simultaneously to the force spectroscopy experiments.
- **C.** The distribution and shape of FAs as well as the shape of the cells selected for following detachment experiments were recorded inside the fluid chamber of the AFM using fluorescence microscopy and phase contrast microscopy. The obtained

micrographs were then used for the quantification of the number, size and area of focal adhesion clusters

The cell projection area *A* is a suitable parameter for the evaluation of the quality of cellular adhesion, as the spreading behavior of fibroblasts crucially depends on the properties of the cellular environment.[32] To analyze *A* and the cell shape, micrographs were recorded by conventional phase-contrast microscopy. Images of cells were taken on the different substrates 6, 12 and 24 hours after seeding. Mean values of the cellular spreading area as a function of time are presented in Figure 2. On all substrates the projected cell area increased with time. On the extensive nanostructured surfaces (**2–4**) smaller spreading area is related to greater ligand spacing, in other words, decreased global ligand density. Six hours after cell seeding the projected cell area was similar on all three of the surfaces with low global ligand densities (**1–3**; $\rho < 212\ \mu m^{-2}$). At the same time it was much larger on the surface with the greatest global ligand density (**4**; $\rho = 355\ \mu m^{-2}$). At this time point there were no considerable differences in the cellular shape on the different substrates (data not shown). Twelve and 24 hours after seeding the effect of local particle density began to show: the spreading area of cells on the two surfaces with an inter-ligand spacing of 57 nm (**1**, **4**) was significantly larger than on the surfaces with ligands spaced apart more than 70 nm. By then, on latter substrates we determined remarkably less viable cells. After 24 h the number of adherent cells was only 5–20% of the number of cells adhering to substrates featuring an inter-ligand spacing of around 57 nm, even though the number of initially seeded cells had been roughly the same. Moreover, the agile and still adherent cells on substrates **(2)** and **(3)** displayed more filopodial structures than on substrate (**1**) and (**4**).

These data suggest that cells discriminate between low, i.e., $< 211\ \mu m^{-2}$, and high, i.e., $> 211\ \mu m^{-2}$, global ligand density regarding their projected cell area within the first 6 hours. The local ligand density has little influence on the projected cell area in this time frame. These results are in line with experiments performed on substrates featuring insufficient fibronectin concentrations.[33] Only after 12 hours do cells start to discriminate between differences in local ligand density. Cell spreading is more successful on all surfaces where ligands are spaced less than circa 60 nm apart, although it is still affected by global ligand density such that cells spread best on an extensive, uniformly patterned surface. In numbers the effect of global ligand density can be described as follows: After 24 h of growth on the micro-nanopatterned surface (**1**) the mean projected cell area adds up to about 80% of the area on surface (**4**), although the number of ligands presented on surface (**1**) are less than 20% of those on surface (**4**). In contrast, surfaces (**2**) and (**3**) were clearly much more difficult for cells to adhere to and especially after 12 and 24 hours the number of adhesive cells was substantially less than on surfaces **(1)** and **(4)**. Conversely, this also suggests that those cells able to adhere to surfaces **(2)** and **(3)** were either more robust than those unable to or were situated on defect structures, meaning either the passivation had locally peeled off or an irregularity during production had resulted in an unintended accumulation of biofunctionalized gold particles. Such a defect could also explain why the cell spreading area on surfaces exhibiting a ligand spacing greater than 60 nm continues to increase between 12 h and 24, just like on surfaces (**1)** and (**4)**. To see whether the spreading area values after 24 hours are different to each other we applied the Welch's t test for unpaired two samples with possibly unequal variances. The null hypothesis in our case was that the spreading area values of two given surfaces after 24 h are equal. This test yielded a p-value $< 0{,}01$ for every neighboring value of spreading area after 24 hours, which gives evidence sufficient to reject the null hypothesis. This means that with a chance of more than 99% that the alternative hypothesis, which states that the mean values of all spreading areas after 24 hours are different, is true. The graph also allows a simple visual assessment concerning the significance of global versus local ligand density for cell spreading. On the far right the four surfaces are labeled, and thus placed in order from top to bottom according to how well cells

can spread on them after 24 hours. At a glance it is noticeable that the difference between surfaces (**2**, **3**) and surface (**4**) (effect of local ligand density) is greater than between surface (**1**) and (**4**) (effect of global ligand density).

The stability of adhesion clusters under constant force was first modeled by Bell [34] and many recent theoretical studies are based on a stochastic version of this model.[35, 36] The model described in these publications assume that receptor-ligand bonds are clustered on opposing surfaces, of which the upper one transmits a constant force homogeneously onto the array of bonds. This force is responsible for the rupture of closed bonds, while at the same time open bonds can close again with a force-independent rebinding rate, stabilizing the adhesion cluster. The rupture of bonds between the two surfaces ultimately leads to an increase of force on the remaining intact bonds. The critical force F_C, also referred to as the stall force, is the threshold force above which adhesion bonds rupture without rebinding, leading to disintegration of the cluster. Thus, the adhesion force F_{ADH}, which is measured by quantifying the force necessary to break all cell-surface contact points and to completely disassociate the cell from the substrate, is equal to the critical force F_C. In their work Schwarz et al. [34] speculate that focal adhesions might be regulated to exist under a force that is very close to the critical force because this would allow small changes in cytoskeletal loading to directly affect and accelerate cluster dynamics.

To quantify adhesion forces involved in cell-substrate interaction processes single cell force spectroscopy (SCFS)[37] was applied. The experimental principle of SCFS is explained in Figure 3. For a more detailed description of the technique and data evaluation process see the publication of Selhuber-Unkel et al. [14] There it was shown that an internal rupture force as result of a vertical pulling force seems to be an universal property of focal adhesions. They found that the cell detachment force increases with increasing ligand density. But interestingly in a certain regime the increase of force was significantly higher than the increase of available ligands. On substrates presenting ligands 90 nm spaced apart the force was relatively small but it strongly increased as soon as the underlying substrate presented ligands spaced 50 nm. This was explained again by findings of Arnold et al. that most probably there is a critical limit (between 50 and 90 nm) in terms of ligand spacing above which formation of stable focal adhesion is inhibited causing also a collapse of the detachment force.

For the experiments cells were cultured on the patterned substrate for 12 hours. A tipless cantilever was functionalized by covalently binding a capture probe (in our case fibronectin) and brought into contact with a cell of interest for about 10–15 minutes to establish a stable cell-cantilever connection. The cell was slowly ruptured from the surface and the force acting on the cell at each time-point was determined by the vertical deflection of the cantilever with a known spring constant. The sum of all vertical force steps F_{tot}, as monitored in the force-distance curve (Figure 3b), equals the complete rupture force F_{ADH}. Simultaneous phase and fluorescence microscopy ensured that every cell was detached properly from the surface (Figure 3a).

Parallel to performing the cantilever experiments, fluorescence microscopy images of cells attached to substrates (**1–4**) were taken (Figure 4). Such images were used for the quantitative analysis of the number and area of focal adhesion clusters (see below).

Figure 4 shows typical fluorescence micrographs of REF-YFP-Pax cells seeded on differently patterned substrates (**1–4**). Monitoring of the aggregated Paxillin-YFP proteins by fluorescent optical microscopy reveals bright spots at the rim of the projected cell area, which represent contact areas (FAs) of the cell with the substrate (top row). Image processing was applied to enhance visibility of contact sites in order to precisely quantify

the number and area of adhesion sites (for details see Supplementary Information and Error Discussion). Figure 4.1 shows that cells spread well on 57 nm spaced micro-nanostructured surfaces and form mature FAs, although it is the surface with the lowest global particle density. The FA shape and area reflect the geometry of the micro-nanopattern, in other words, each spot in Figure 4.1 represents one ligand-presenting “island” in the pattern. On surfaces with an inter-ligand spacing greater than 70 nm, FA formation is suppressed (Figure 4.2) or diminished (Figure 4.3). In contrast, cells develop the most pronounced, oblong-shaped contact areas on surface (**4**), which has ligands spaced 57 nm apart (Figure 4.4).

Figure 5 shows how the values obtained through single cell force spectroscopy and quantitative optical microscopy inside the AFM fluid chamber 12 hours after cell seeding relate to global ligand density.

The number of FAs and their size was quantified for each cell and average values for each surface type were calculated (Figure 5a). Regarding the size of individual fibroblast FAs, descriptions in literature range from one to 15 μm^2. For instance, Balaban et al. determined FAs containing vinculin and paxillin of foreskin and cardiac fibroblasts to be between 1–10 μm^2 [38] in size and Franz et al. in their analysis of FAs with the atomic force microscope observed oblong structures sized 0.5–2 μm × 3–8 μm.[39] In our case shape, size and number of established focal adhesions were influenced by the surface pattern (Figure 4.1–4.4 and Figure 5a). The micro-structuring of a substrate does not seem to limit the number of FAs a cell can develop. On the contrary we observed a slight tendency of cells to establish more FAs in an attempt to antagonize the restrictions they encounter on surface (**1**). Most FA only occupied a single adhesive circular patch with a diameter of around 2 μm^2 (visible in (Figure 4.1)). The average value of around 3 μm^2 for FA sizes in Figure 5a results from a few larger FA patches, where cells were able to bridge non-adhesive areas. On extensive, uniformly nanopatterned substrates (**2–4**) the number and area of FAs increase with increasing ligand density. Accordingly, cells on substrate (**4**) had the most and the largest FAs.

Figure 5b shows the entire area of FA clusters per cell as a function of global ligand density. In our experiments cells on surfaces with ligands spaced apart more than 60 nm (**2, 3**) featured a smaller FA area than cells on surfaces with more densely spaced ligands (**1, 4, 5**). This speaks for the existence of a threshold value for inter-ligand spacing with regard to cell spreading, which we fix at approximately 60 nm. In Figure 5b) and 5c) we included data from a previous publication, measured on a surface (henceforth termed surface **(5)**) with ligands spaced only 28 nm apart and a global ligand density much higher than any of the other surfaces ($\rho \sim 1473\ \mu m^{-2}$). The focal adhesion area of cells on surface (**5**) is very similar to that of surface **(4)**, which suggests that on extensive nanopatterned surfaces the FA area, when plotted for increasing ligand density, seems to follow a saturation curve.

The number of established focal adhesions and the entire adhesive area provide information about the cell’s ability to form cell-ECM connections. With this data it is possible to make assumptions about which nanoscopic properties of the ECM act to support, impair or even inhibit cell adhesion.

Figure 5c shows the relationship of the adhesive area of each cell to its corresponding absolute detachment force (inset), also referred to as the adhesion force density ρ_{ADH}. The cells on surface (**4**) display the highest absolute detachment force compared to surfaces (**1–3**). The absolute detachment force of cells seeded on the micro-nanostructured surface (**1**) was more than half the value (F~420 nN) of that on surface (**4**), while on extensive nanostructured surfaces with ligands spaced more than 60 nm apart (**2**, **3)** it is less than one sixth of the value of surface (**4**). Because both the adhesion force and the focal adhesion area

correlate with global ligand density in the same way (the less ligands per μm^2 a surface has, the less adhesive forces are needed to detach cells from it and the less adhesive area can be found on these cells), you would expect the adhesion force density of all surfaces to be alike. Instead, the data revealed that on the micro-nanostructured surface adhesion force densities are almost as high as on extended patterns with the same ligand spacing. In contrast, the absolute adhesion force on surface (**2**), which has a distance of 120 nm between ligands, is close to zero, suggesting that FAs are less stable in this case (also see below). Surface (**5**), after biofunctionalization with fibronectin, displayed an absolute detachment force of $F \sim 1100$ nN.[14] By including these data in Figure 5c, it becomes apparent that the adhesion force density on extensive nanopatterned surfaces, when plotted for increasing ligand density again seems to follow a saturation curve. In contrast, such a relationship (reduced global density leading to a reduced adhesion force) was not found for micro-nanostructured substrates.

The influence of global versus local ligand density, as measured in the experiments above, can be summarized by comparing the overall characteristics of cell adhesion of the surfaces in two separate groups, the first consisting of surfaces (**2–5**) and the second including only surfaces (**1**) and (**4**). Considering surfaces (**2–5**) shows that among uniform, extensive substrates all values that serve to quantify adhesion strength and the ability to adhere (the number and size of adhesions as well as the adhesion force density) are smaller on surfaces with less ligands per μm^2. Furthermore, as mentioned above, the curves relating FA area, F_{ADH} and ρ_{ADH} to ligand densities for surface (**2**)-(**5**) climax over time. Although our experimental design does not allow us to prove that an upper limit for each of these three parameters exists, nevertheless, it is clearly visible that the slopes of these curves level out as ligand density increases.

In summary, the FA area, F_{ADH} and ρ_{ADH} of investigated cells on surfaces (**2–5**) exceeding a certain ligand density parameterize a stable adhesion regime. The boundary condition of this regime is an inter-ligand spacing of around 60 nm on the adhesive surface. Below this limit all three parameters constantly decrease down to ultimate failure of cells to adhere (no ligands-no adhesion). All surfaces where the above-mentioned parameters (FA area, F_{ADH} and ρ_{ADH}) have values that lie within the steeply accelerating part of the slope (namely surfaces (**2**)–(**4**)) follow the rule that the lower the ligand density - the lower the FA area, F_{ADH} and ρ_{ADH}. An exception to this rule is the micro-nanostructured surface **(1)**, whose properties are closest in resemblance to those of surface **(4)**, which has the same local ligand density. So, as cell adhesion behavior on surfaces (**1**,**4**) is very similar the local density rather than the global ligand density must be dominant in its influence on parameters describing cell adhesion.

Conversely, it can be concluded that the formation of strong adhesive protein clusters requires extracellular adhesive ligands to be spaced closer than the critical value of around 60 nm. But why are cells restricted in their ability to adhere to surfaces with ligands that are spaced further apart than a certain threshold level? The binding strengths of the receptors as well as their number and geometric placement determine at what force the cell will start to detach. Therefore, decreased adherence can be related to a decrease in the number of anchor points or their stability. The first assumption can be excluded based solely on the fact that surface (**1**), the surface with the lowest number of overall ligands available to a cell, has more and larger FAs as well as a greater adhesion force density than surface (**2**) or (**3**). This allows the conclusion that the distance between ligands affects the stability and strength of focal adhesions. The stability of FAs is closely related to the dynamic processes of focal adhesion initiation, assembly, maturation and disassembly. The development from an initial adhesion to a focal complex and the following maturation into a focal adhesion is marked by the recruitment of numerous proteins, starting with integrin and some adapter proteins like

talin and paxillin in focal complexes. Many focal complexes fail to mature and are disassembled, but some continue to mature and grow, accompanied by the recruitment of additional proteins, such as zyxin and tensin.[31] Facts supporting the thesis that FAs fail to mature on surface (**2**) and (**3**) are: (i) the shape of FAs in the fluorescence micrographs (Figure 4), where surface (**2**) has none, surface (**3**) only rudimentary and surface (**4**) oblong-shaped FAs and (ii) the size of FAs. From this we can deduce that the differences in the maturation state, and consequentially the molecular composition of FAs, is most likely the reason for the reduction in adhesion force density on surfaces with ligands spaced more than approximately 60 nm apart.

The comparison of surfaces (**1**) and (**4**), on the other hand, shows that a patterned microstructure, which allows adhesion only on ligand-displaying islands, results in a lower number and a smaller size of bound adhesion receptors (leading to a reduced FA area) and subsequently a lower total detachment force. Again, the question arises of whether this is caused by a decrease in the ligand number or a decrease in the stability of the FAs. The fluorescence micrographs in Figure 3 show the existence of numerous FAs on surface (**1**), although they differ in shape to those on surface (**4**). These pictures suggest that the size of FAs on surface (**1**) reflect the exact size of the micro-patches. Although, cells on surface (**1**) have a comparable number of FAs connecting the cell to the surface (**4**), the focal adhesion area is smaller. This suggests, that although surface (**1**) has less than a fifth of the number of ligands of surface (**4**), cells attempt to attach to the micro-patterned surface through focal adhesions. But, because the completion of growth (and subsequently also the maturation) of functional FAs is limited by the size of the adhesive islands, the adhesion force of cells on surface (**1**) is weaker than that of cells on surface (**4**). Nonetheless, although micro-structuring of the substrate may affect the stability and strength of cell adhesion, this effect is much weaker than on substrates (**2**) and (**3**) where many cells are unable to attach at all.

In this work we took a nano-scale look at focal adhesions, the anchorage points of cells as they adhere to the ECM. We introduced a novel facet to investigating the influence of ligand density on cell adhesion strength and focal adhesion formation by distinguishing between local ligand density, i.e. ligand spacing, and global ligand density. Precise control of ligand presentation - spacing and density - was obtained by defining micro- and nanostructured gold arrays on glass cover slides as ligand anchors. The number of available anchor points determines the strength of the entire cell-matrix connection, however, our results imply that single focal adhesion clusters are only stable when ligands are spaced below a critical value. Limiting the number of available anchor points by micro-nanostructuring results in smaller established adhesion sites and entire adhesion area, but increasing the distance between the ligands leads to unstable and weak FA clusters and can even inhibit the development of FAs from focal complexes.

Supplementary Material

Refer to Web version on PubMed Central for supplementary material.

Acknowledgments

We thank A. Cavalcanti-Adam, C. Böhm, H. Böhm and B. Maddes for fruitful discussions. The work was greatly structured and corrected by N. Grunze. The Max Planck Society is acknowledged for its general support. The work was supported by the National Institutes of Health through the NIH Roadmap for Medical Research (PN2 EY016586). The research leading to these results has received partly funding from the European Union Seventh Framework Programme (FP7/2007-2013) under grant agreement n° NMP4-LA-2009-229289 NanoII and under grant agreement n° NMP3-SL-2009-229294 NanoCARD.

References

1. Vogel V, Sheetz M. Local force and geometry sensing regulate cell functions. Nature Reviews Molecular Cell Biology. 2006; 7(4):265–275.
2. Zaidel-Bar R, Itzkovitz S, Ma'ayan A, Iyengar R, Geiger B. Functional atlas of the integrin adhesome. Nat Cell Biol. 2007; 9(8):858–67. [PubMed: 17671451]
3. Geiger B, Spatz JP, Bershadsky AD. Environmental sensing through focal adhesions. Nat Rev Mol Cell Biol. 2009; 10(1):21–33. [PubMed: 19197329]
4. Geiger B, Yehuda-Levenberg S, Bershadsky A. Molecular interactions in the submembrane plaque of cell-cell and cell-matrix adhesions. Acta anatomica. 1995; 154:46–62.
5. Chen CS, Mrksich M, Huang S, Whitesides GM, Ingber DE. Geometric control of cell life and death. Science. 1997; 276(5317):1425. [PubMed: 9162012]
6. Zajac AL, Discher DE. Cell differentiation through tissue elasticity-coupled, myosin-driven remodeling. Current Opinion in Cell Biology. 2008; 20(6):609–615.
7. Geiger B, Bershadsky A, Pankov R, Yamada KM. Transmembrane crosstalk between the extracellular matrix and the cytoskeleton. Nature Reviews Molecular Cell Biology. 2001; 2(11): 793–805.
8. Engler AJ, Sen S, Sweeney HL, Discher DE. Matrix elasticity directs stem cell lineage specification. Cell. 2006; 126(4):677–689.
9. Zaidel-Bar R, Itzkovitz S, Ma'ayan A, Iyengar R, Geiger B. Functional atlas of the integrin adhesome. Nature cell biology. 2007; 9(8):858–867.
10. Hynes RO. Integrins: versatility, modulation, and signaling in cell adhesion. Cell. 1992; 69(1):11–25.
11. Massia S, Hubbell J. An RGD spacing of 440 nm is sufficient for integrin alpha V beta 3-mediated fibroblast spreading and 140 nm for focal contact and stress fiber formation. Journal of Cell Biology. 1991; 114(5):1089–1100.
12. Arnold M, Cavalcanti-Adam EA, Glass RJB, Eck W, Kantlehner M, Kessler H, Spatz JP. Activation of integrin function by nanopatterned adhesive interfaces. Chemphyschem. 2004; 5(3): 383–388.
13. Cavalcanti-Adam EA, Micoulet A, Bluemmel J, Auernheimer J, Kessler H, Spatz JP. Lateral spacing of integrin ligands influences cell spreading and focal adhesion assembly. Eur J Cell Biol. 2006; 85(3–4):219–224.
14. Selhuber-Unkel C, Erdmann T, López-García M, Kessler H, Schwarz U, Spatz J. Cell Adhesion Strength Is Controlled by Intermolecular Spacing of Adhesion Receptors. Biophysical Journal. 2010; 98(4):543–551.
15. Arnold M, Schwieder M, Blümmel J, Cavalcanti-Adam E, López-Garcia M, Kessler H, Geiger B, Spatz J. Cell interactions with hierarchically structured nano-patterned adhesive surfaces. Soft Matter. 2009; 5(1):72–77.
16. Huang J, Grater S, Corbellini F, Rinck S, Bock E, Kemkemer R, Kessler H, Ding J, Spatz J. Impact of order and disorder in RGD nanopatterns on cell adhesion. Nano Lett. 2009; 9(3):1111–1116.
17. Wei Y. Physical Interpretation of the Maximum Receptor- Ligand Bond Spacing to Ensure Cell Adhesion in Ligand-Coated Substrates. Langmuir. 2008; 24(11):5644–5646.
18. de Beer A, Cavalcanti-Adam E, Majer G, Lopez-García M, Kessler H, Spatz J. Force-induced destabilization of focal adhesions at defined integrin spacings on nanostructured surfaces. Physical Review. 2010; E 81(5):51914.
19. Aydin D, Schwieder M, Louban I, Knoppe S, Ulmer J, Haas TL, Walczak H, Spatz JP. Micro-nanostructured protein arrays: a tool for geometrically controlled ligand presentation. Small. 2009; 5(9):1014–1018. [PubMed: 19242941]
20. Spatz JP, Roescher A, Sheiko S, Krausch G, Moller M. Noble metal loaded block lonomers: micelle organization, adsorption of free chains and formation of thin films. Advanced Materials. 1995; 7(8)
21. Glass R, Moller M, Spatz JP. Block copolymer micelle nanolithography. Nanotechnology. 2003; 14(10):1153–1160.

22. Lussi JW, Falconnet D, Hubbell JA, Textor M, Csucs G. Pattern stability under cell culture conditions—a comparative study of patterning methods based on PLL-g-PEG background passivation. Biomaterials. 2006; 27(12):2534–2541. [PubMed: 16364431]
23. Lee JH, Lee HB, Andrade JD. Blood compatibility of polyethylene oxide surfaces. Progress in Polymer Science. 1995; 20(6):1043–1079.
24. Pfaff M, Tangemann K, Muller B, Gurrath M, Muller G, Kessler H, Timpl R, Engel J. Selective recognition of cyclic RGD peptides of NMR defined conformation by alpha IIb beta 3, alpha V beta 3, and alpha 5 beta 1 integrins. Journal of Biological Chemistry. 1994; 269(32):20233. [PubMed: 8051114]
25. Kantlehner M, Schaffner P, Finsinger D, Meyer J, Jonczyk A, Diefenbach B, Nies B, Hölzemann G, Goodman S, Kessler H. Surface coating with cyclic RGD peptides stimulates osteoblast adhesion and proliferation as well as bone formation. Chembiochem. 2000; 1(2):107–114. [PubMed: 11828404]
26. Fratzl P, Misof K, Zizak I, Rapp G, Amenitsch H, Bernstorff S. Fibrillar structure and mechanical properties of collagen. Journal of Structural Biology. 1998; 122(1–2):119–122.
27. Jiang X, Wang X. C YTOCHROME C-M EDIATED A POPTOSIS. Annual review of biochemistry. 2004; 73(1):87–106.
28. Meller D, Peters K, Meller K. Human cornea and sclera studied by atomic force microscopy. Cell and tissue research. 1997; 288(1):111–118. [PubMed: 9042778]
29. Cavalcanti-Adam EA, Volberg T, Micoulet A, Kessler H, Geiger B, Spatz JP. Cell spreading and focal adhesion dynamics are regulated by spacing of integrin ligands. Biophys J. 2007; 92(8): 2964–2974.
30. Cavalcanti-Adam, EA.; Aydin, D.; Hirschfeld-Warneken, VC.; Spatz, JP. Cell adhesion and response to synthetic nanopatterned environments by steering receptor clustering and spatial location. 2008.
31. Zaidel-Bar R, Ballestrem C, Kam Z, Geiger B. Early molecular events in the assembly of matrix adhesions at the leading edge of migrating cells. Journal of Cell Science. 2003; 116(22):4605–4613.
32. Yeung T, Georges P, Flanagan L, Marg B, Ortiz M, Funaki M, Zahir N, Ming W, Weaver V, Janmey P. Effects of substrate stiffness on cell morphology, cytoskeletal structure, and adhesion. Cell motility and the cytoskeleton. 2005; 60(1):24–34.
33. Dubin-Thaler BJ, Giannone G, Doebereiner HG, Sheetz MP. Nanometer analysis of cell spreading on matrix-coated surfaces reveals two distinct cell states and STEPs. Biophysical journal. 2004; 86(3):1794–1806.
34. Bell G. Models for the specific adhesion of cells to cells. Science. 1978; 200(4342):618.
35. Erdmann T, Schwarz U. Stability of adhesion clusters under constant force. Physical review letters. 2004; 92(10):108102.
36. Schwarz US, Erdmann T, Bischofs IB. Focal adhesions as mechanosensors: the two-spring model. BioSystems. 2006; 83(2–3):225–232.
37. Helenius J, Heisenberg CP, Gaub HE, Muller DJ. Single-cell force spectroscopy. Journal of Cell Science. 2008; 121(11):1785.
38. Balaban NQ, Schwarz US, Riveline D, Goichberg P, Tzur G, Sabanay I, Mahalu D, Safran S, Bershadsky A, Addadi L, et al. Force and focal adhesion assembly: a close relationship studied using elastic micropatterned substrates. Nature Cell Biology. 2001; 3(5):466–472.
39. Franz C, Muller D. Analyzing focal adhesion structure by atomic force microscopy. Journal of Cell Science. 2005; 118(22):5315–5324.
40. Cleveland J, Manne S, Bocek D, Hansma P. A nondestructive method for determining the spring constant of cantilevers for scanning force microscopy. Review of Scientific Instruments. 1993; 1(2):5.

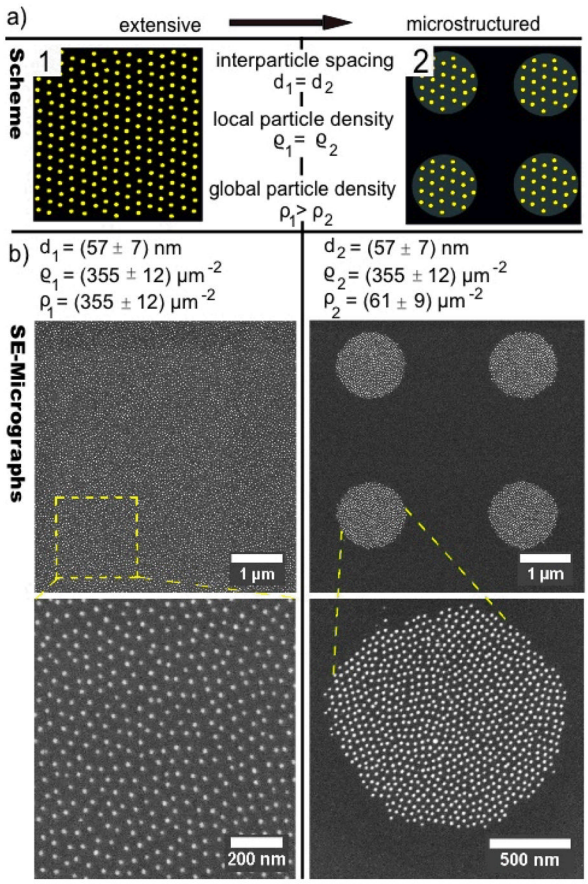

Figure 1.

(a) The scheme shows that hierarchically organized nanoparticle arrays in microdomains allow for the separation of local particle density (interparticle distance) from global particle density. (b) Scanning electron micrographs of representative nano- and micro-nanopatterned surfaces used for experiments. The surfaces in the left and in the right column both have the same local particle density, but differ in their global particle density. The bottom pictures show enlarged details.

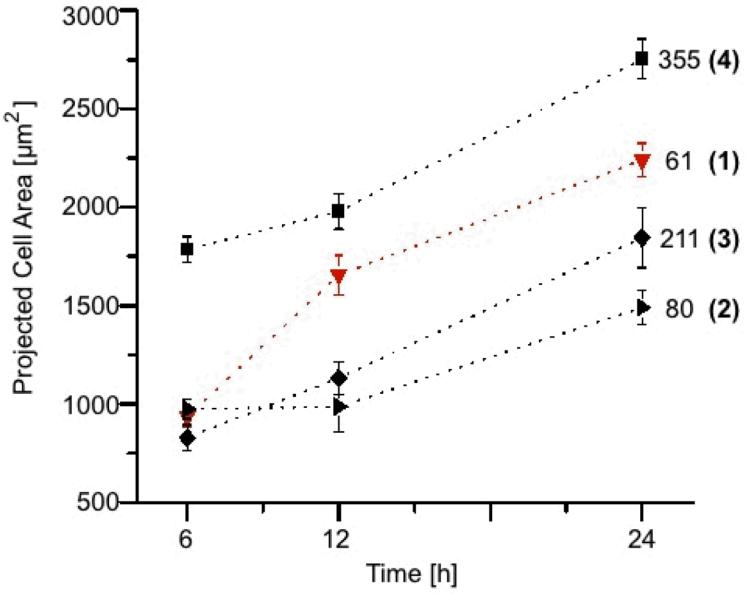

Figure 2.

Cellular spreading area of cells on substrates with different ligand densities after 6, 12 and 24 h of cell-substrate interaction, respectively (substrate numbers 1–4 given in parentheses on far right). Global ligand densities, given in μm^{-2}, are listed next to substrate numbers. The red data points highlight the results of cells on substrate number one, the micro-nanostructured surface with the smallest global ligand density but a high local ligand density. The values are mean values with corresponding standard error of the mean. (6h: n_1= 28; n_2= 54; n_3=21; n_4=23; 12h: n_1= 29; n_2= 34; n_3=24; n_4=32; 24h: n_1= 39; n_2=34; n_3=18; n_4=50)

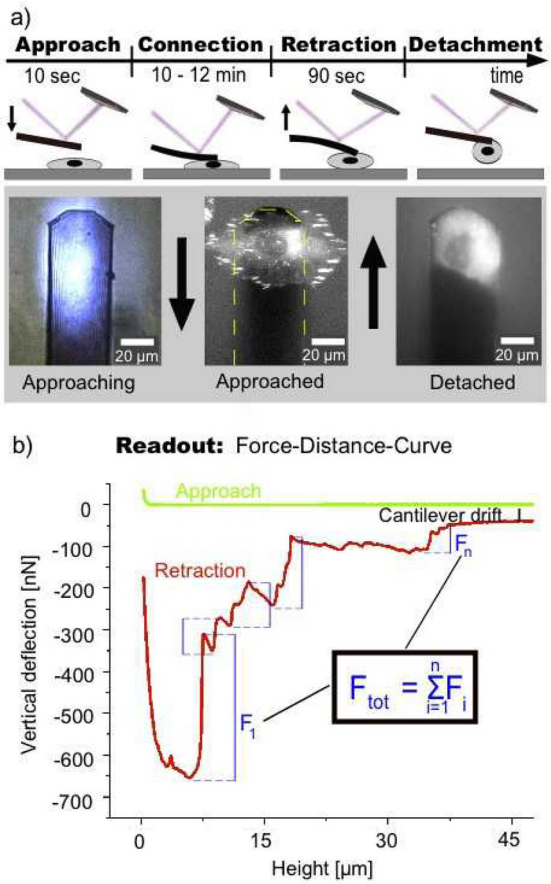

Figure 3.

The principle of SCFS. (a) Approach: a fibronectin-coated cantilever is immobilized on an adherent cell from above; Connection: a stable connection between the capture probe and the target molecule is established; Retraction: The cantilever is retracted with a constant pulling rate, leading to nanomechanical bending of the cantilever; Detachment: the cantilever-bound cell is detached from the substrate and the deflection of the cantilever recorded. The bottom row shows fluorescence micrographs of the cell in contact with the cantilever during (i) approach, (ii) contact, and (iii) after detachment from the nanopattern surface. The middle micrograph presents focal adhesions as white stripes. (b) The force-distant curve provides information on the force magnitudes related to the breaking and manipulation of chemical bonds during the detachment process.

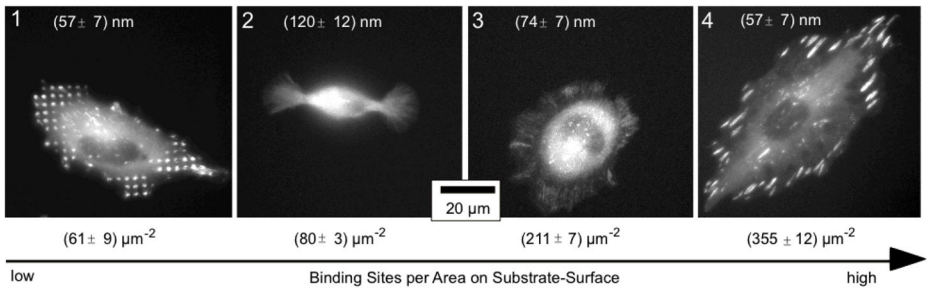

Figure 4.

Micrographs of REF-YFP-Pax cells 12 h after seeding on micro-nanostructured surfaces (1) or extensive nanopattern surfaces with different inter-ligand spacings (given in parentheses) (2–4). Focal adhesions (visible as bright patches on the cell periphery) develop well on substrates with an inter-ligand spacing of less than 70 nm (1, 4). Underneath the global particle density for each surface is given.

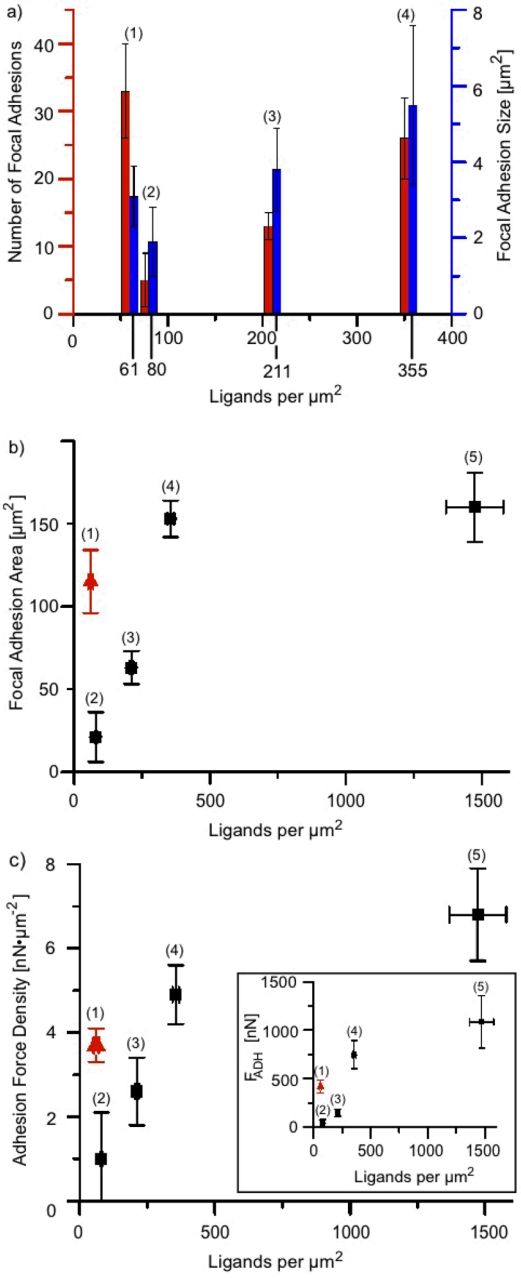

Figure 5.

Focal adhesion number, size, area and their adhesion force as a function of global ligand density (for each data point five cells were evaluated except for surface **(5)** (see below); the error bars correspond to the standard errors of the mean): (a) number of FAs equal to or greater than 1 μm^2 (red) and their mean size (blue) (surface numbers are given in parentheses above columns). To visualize the development of the data for high ligand densities in **b** and **c** previously published data points of an additional surface with a spacing of around 28 nm ($\rho \sim 1473\ \mu m^{-2}$)[14] were added. (b) The total mean area of FAs per single cell. (c) The adhesion force density (ρ_{ADH}) was calculated by relating the absolute detachment force (inset (c)) to the total area of FAs. Red data points (triangles) represent data obtained on the micro-nanostructured surface (1).

Table 1

Parameters of the nano-and micro-nanostructured surfaces

Pattern Type	#	Particle Spacing *d* [nm]	Local Particle Density ρ [μm^{-2}]	Global Particle Density ρ [μm^{-2}]
micro-nano	**1**	57 ± 7	355 ± 12	61 ± 9
extensive	**2**	120 ± 15	80 ± 3	80 ± 3
extensive	**3**	74 ± 7	211 ± 7	211 ± 7
extensive	**4**	57 ± 7	355 ± 12	355 ± 12